NASA Technical Memorandum 103861

Computer Aiding for Low-Altitude Helicopter Flight

Harry N. Swenson

May 1991

National Aeronautics and Space Administration

NASA Technical Memorandum 103861

Computer Aiding for Low-Altitude Helicopter Flight

Harry N. Swenson, Ames Research Center, Moffett Field, California

May 1991

National Aeronautics and
Space Administration

Ames Research Center
Moffett Field, California 94035-1000

SUMMARY

A computer-aiding concept for low-altitude helicopter flight has been developed and evaluated in a real-time piloted simulation. The concept included an optimal control trajectory-generation algorithm based on dynamic programming, and a head-up display (HUD) presentation of a pathway-in-the-sky, a phantom aircraft, and flight-path vector/predictor symbol. The trajectory-generation algorithm uses knowledge of the global mission requirements, a digital terrain map, aircraft performance capabilities, and advanced navigation information to determine a trajectory between mission waypoints that minimizes threat exposure by seeking valleys. The pilot evaluation was conducted at NASA Ames Research Center's Sim Lab facility in both the fixed-base Interchangeable Cab (ICAB) simulator and the moving-base Vertical Motion Simulator (VMS) by pilots representing NASA, the U.S. Army, and the U.S. Air Force. The pilots manually tracked the trajectory generated by the algorithm utilizing the HUD symbology. They were able to satisfactorily perform the tracking tasks while maintaining a high degree of awareness of the outside world.

INTRODUCTION

Helicopters that operate in threat areas have a need for low-level, maneuvering-penetration capability under nighttime and adverse weather conditions. Currently, this low-level penetration is accomplished through terrain-following (TF) systems by using a combination of technologies such as multimode radar (MMR) systems, forward-looking infrared (FLIR), and night-vision goggles (NVG). TF systems were initially developed for fixed-winged tactical and strategic aircraft such as the FB-111 and B-1B. The TF systems have also been developed for combat search and rescue aircraft such as the CH-53 PAVE LOW III and the HH-60 helicopters, and are currently part of the Army's Special Operations Forces (SOF) helicopters (ref. 1). The TF systems generate vertical commands that are either displayed on a flight director for manual flight or sent to the flight-control system for automatic flight. These systems do not generate commands for lateral maneuvering, are limited to line-of-sight maneuvering, and do not provide information to the pilot that would allow him to make strategic decisions that could give better terrain masking.

Recently the Air Force sponsored research to extend TF capability for high-performance aircraft to include lateral maneuvering by taking advantage of on-board digital terrain data, references 2-5. The work concentrated on the development of four potential algorithms, each of which is based on minimizing a quadratic cost functional, defined to reflect the degree of vulnerability. This extended capability is commonly referred to as terrain-following/terrain-avoidance (TF/TA) in the literature.

Within the last few years there has been considerable work within NASA and elsewhere (refs. 6-8) in applying these algorithms to rotorcraft. The NASA research has concentrated on incorporating these algorithms into an operationally acceptable system, referred to as the Computer Aiding for Low-Altitude Helicopter Flight Guidance System; several piloted simulations of this system have been conducted. The first two were dedicated to the development of the system and pilot interface issues. They are described thoroughly in reference 9.

The purpose of this paper is to present the results of an operational evaluation of the guidance and display concepts developed in reference 9 using the Vertical Motion Simulator (VMS) at Ames. The primary objectives of this simulation were to 1) determine the pilot guidance-tracking performance under various combinations of environmental conditions, terrain, and aircraft speeds, and 2) examine the ability of the pilot to integrate the guidance information with the outside world when visibility allows for pilot-directed obstacle avoidance and improved concealment. The paper is organized so as to familiarize the reader with computer-aiding for low-altitude helicopter flight by describing the overall system, which includes 1) the trajectory-generation algorithm, 2) the trajectory coupler, and 3) the displayed information. The simulation, test procedures, and performance results are then covered.

SYSTEM DESCRIPTION

Shown in figure 1 is a functional block diagram of the computer-aiding for low-altitude helicopter flight system. There are three fundamental components: 1) the trajectory-generation algorithm, which is referred to as Dynapath; 2) the trajectory coupler; and 3) the displayed information. This system has to be integrated with the pilot, the helicopter, and the aircraft sensors. The trajectory-generation algorithm, the trajectory coupler, and the displayed information are discussed below.

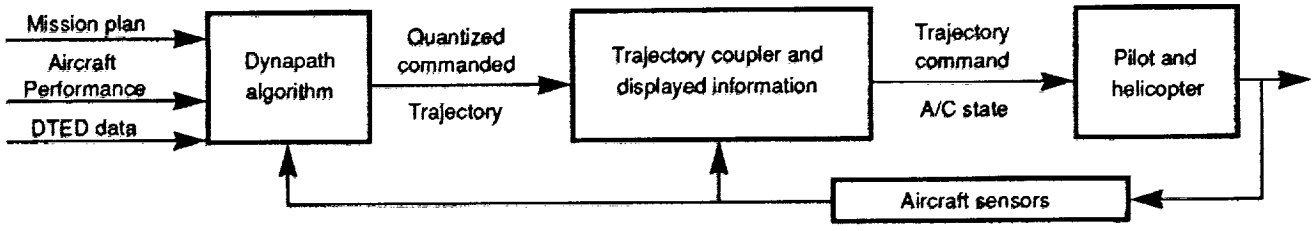

Figure 1. System block diagram.

Trajectory Generation Algorithm

The trajectory-generation algorithm (Figure (1)), known as Dynapath, was originally developed for the U.S. Air Force (ref. 10). The goal of the Air Force research was the development of a TF/TA guidance algorithm for automatic tactical aircraft operations. Significant modifications have been made to this guidance algorithm in adapting it for manual rotorcraft operations. The rationale and description of the modifications are presented in reference (9).

Dynapath is a valley-seeking, trajectory-generating algorithm based on a forward-chaining dynamic-programming technique. In-depth descriptions of Dynapath are provided in references 10 and 11, so it will be treated only briefly here. The algorithm uses two kinds of inputs. The first, characterized as mission-dependent information, includes mission waypoints, for defining a global trajectory to be flown, and Defense Mapping Agency (DMA) digital terrain-elevation data (DTED) of the

area in which the mission is to be accomplished. The second kind of input consists of pilot-comfort and aircraft-dependent information: maximum bank-angle commands, maximum climb and dive angles, maximum pull-up and push-over load factors, set-clearance altitude (desired trajectory altitude above the ground), along with sensed aircraft-state information.

Dynapath uses a decoupled procedure in which the lateral and vertical trajectory solutions are determined independently to obtain an optimal trajectory. In this decoupled procedure, the lateral ground track is first determined by assuming that the aircraft can fly perfectly at the vertical set-clearance altitude. The vertical trajectory is then calculated using the aircraft normal load factor and flight-path angle as maneuver constraints to maintain the aircraft at or slightly above the vertical-set clearance as determined from the digital-terrain map and the lateral ground track.

The lateral path is calculated using a tree structure of possible two-dimensional trajectories by using discretized variation in aircraft bank angle. Assuming constant speed and coordinated flight, each discrete bank value produces a possible path which in combination forms a tree of possible paths (fig. 2). In this implementation, the bank-angle control has five discrete values that are used for the trajectory calculation: ±100% maximum bank angle for large control, ±33% maximum bank angle for fine control, and 0° bank angle. The kinematical relationship for path curvature (ρ) based on the above assumptions is given as

$$\rho = 0,\ \pm\frac{g}{V^2}\tan(\phi_{max}/3),\ \pm\frac{g}{V^2}\tan(\phi_{max}) \tag{1}$$

where

g	acceleration due to gravity
V	aircraft velocity
ϕ_{max}	maximum bank-angle command

At any node point, only three bank-angle control values can be used: the control used in arriving at the node point and the control values to either side. At each successive node of the tree, the aircraft position and heading are stored along with the cumulative cost to each node. The transition equations between each successive node point are

$$\begin{bmatrix} X \\ Y \\ \psi \end{bmatrix}_{n+1} = \begin{bmatrix} \cos(\psi_n) & -\sin(\psi_n) & 0 \\ \sin(\psi_n) & \cos(\psi_n) & 0 \\ 0 & 0 & 1 \end{bmatrix} \times \begin{bmatrix} \frac{1}{\rho}\sin(\rho V\Delta t) \\ \frac{1}{\rho}[1-\cos(\rho V\Delta t)] \\ \rho V\Delta t \end{bmatrix} + \begin{bmatrix} X \\ Y \\ \psi \end{bmatrix}_n \tag{2}$$

where

ρ	path curvature as defined in equation 1
V	aircraft ground speed
Δt	time (1 sec)
ψ	node heading
n	node index

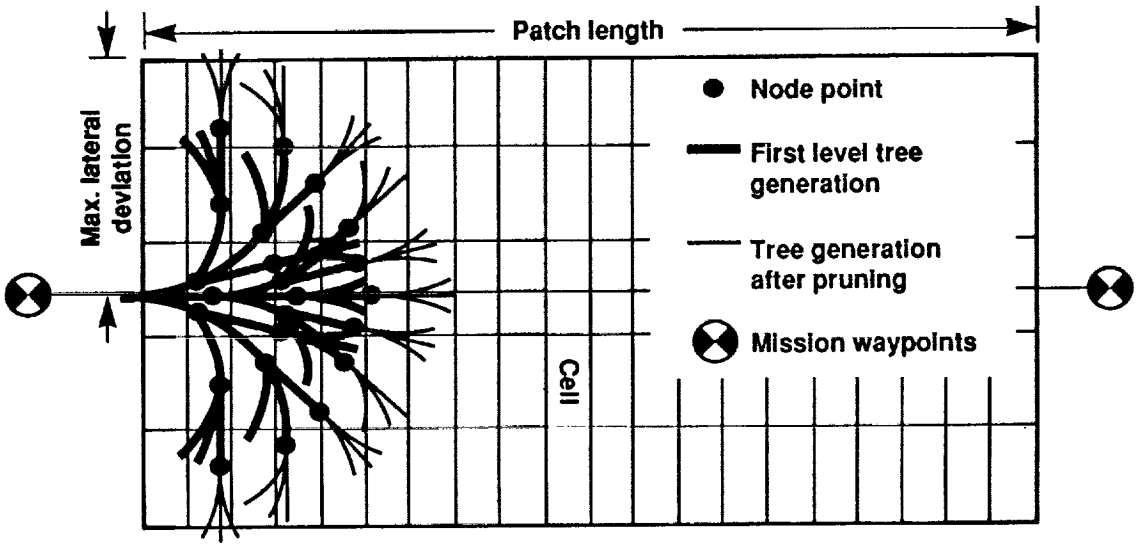

Figure 2. Dynapath tree generation.

A grid is superimposed upon the tree structure with boundaries defined by the maximum lateral deviation and length of optimization. The purpose of the grid is to allow pruning of the tree to keep the amount of possible tree branches at a reasonable level. The size and number of grid elements, or "cells," were determined experimentally in reference 12. For a 30-sec patch the number of cell divisions is 20 longitudinally along the patch and 20 laterally across the patch. Pruning the tree after three to four levels of branching gave the best mix of branch generation and computational speed based on results from nonreal-time computer simulations (ref. 12). Pruning is accomplished by comparing nodes within a cell that are heading in approximately the same direction and choosing the one with the lowest cost to continue the branch propagation. Pruning is also executed on branches that travel outside the grid or in a direction that causes significant path reversals; it is done at each node generation. After the tree structure of possible paths has been propagated through the entire patch length, the cumulative costs of all surviving branches are compared, and the path with the lowest cost is selected as the optimal trajectory.

The cost function J is the performance measure used to determine the optimal trajectory:

$$J = \sum_{i=1}^{30} H_i^2 + f(D)\omega D_i^2 + \alpha(\Delta\psi_i)^2 \tag{3}$$

where

H_i altitude above mean sea level at node i

D_i lateral distance from reference path at node i

ω TF/TA ratio

f(D) dead band on lateral deviation cost, i.e., if $|D| < \delta$ then $f(D) = 0$ where δ is a meaningful distance, else $f(D) = 1$, and $D_i^2 = (D_i - \delta)^2$

$\Delta\psi_i$ the difference between the reference heading and the commanded heading at node i

α heading weight

The rationale for this particular cost functional is given in reference 9, but a brief description is warranted here. The fundamental parameters in this performance measure are the terms representing altitude H and reference-path deviation D. The cost-functional, when driven by these two terms, allows lateral maneuvering to seek lower altitude terrain by the cost reduction from H; excessive deviation from the reference path is controlled by increasing cost due to D. The TF/TA ratio ω allows blending of these two terms to obtain a desired balance between vertical and horizontal maneuvering. The f(D) and $\alpha(\Delta\psi_i)$ terms were added to reduce undesirable oscillations in the trajectory about the nominal path within a patch that are caused by the bank-angle quantization. The f(D) term eliminates the need for precise following of the nominal, or reference, path, and the $\alpha(\Delta\psi_i)$ term provides a penalty for changing the heading from that given by the reference path. These two terms were added based on results from piloted simulations to assist the trajectory-generation algorithm emulate pilot control strategies for low-altitude maneuvering flight (ref. 9).

The trajectory-generation algorithm, as defined above, is designed to compute guidance for a patch that represents the area in front of the aircraft's present location. The patch width is the maximum lateral deviation, and its length is the flight preview distance. Both are input parameters selected by the user. The algorithm is computationally intensive; for example, when using representative values for patch length (≈30 sec) and maximum lateral deviation (≈1 km) the computational cycle is about 4 to 5 sec for a modern flight computer. Several methods for updating and propagating the algorithm were developed and evaluated during piloted simulations (ref. 9). The preferred method is shown pictorially in figure 3. The algorithm is initialized to a predicted location of the aircraft that is one computational cycle from its current position by using

$$\vec{X}_{p_1} = \dot{\vec{X}}_a \cdot t_u + \vec{X}_a \tag{4}$$

where

$\vec{X}_{p_1}$ initial predicted aircraft location

$\dot{\vec{X}}_a$ current aircraft velocity vector

t_u computational cycle time or update time

$\vec{X}_a$ current aircraft location

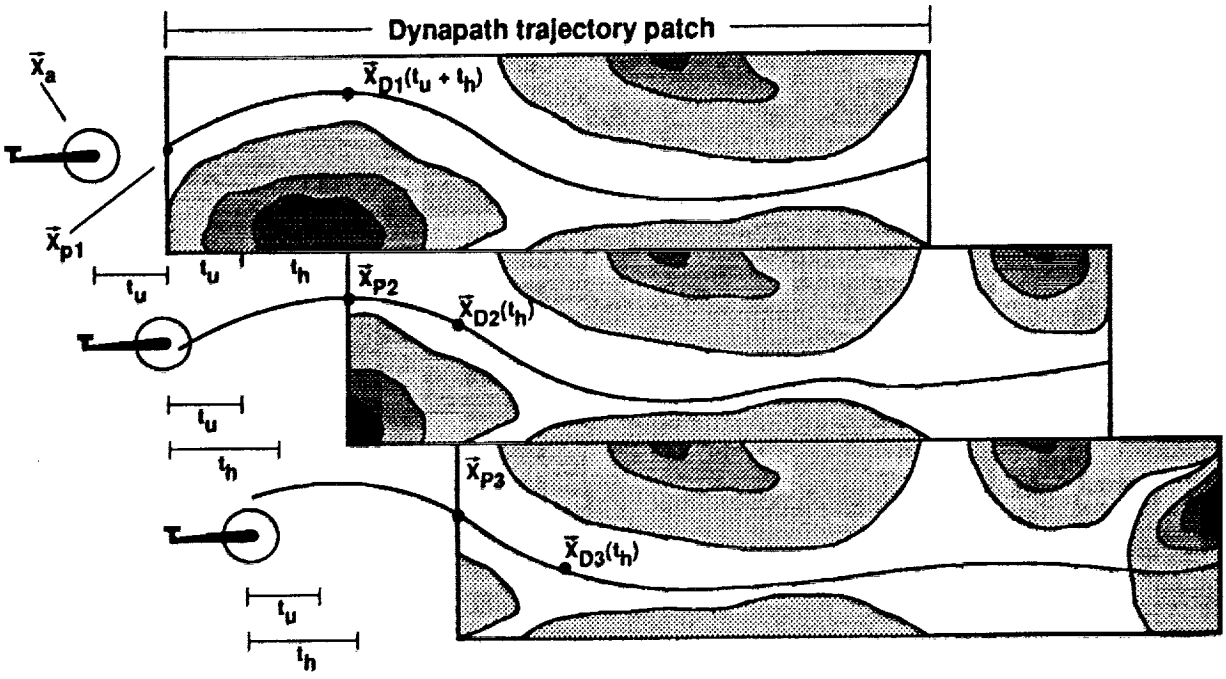

Figure 3. Update procedure.

After $\vec{X}_{p_1}$ is determined, the trajectory-generation algorithm calculates the first patch. Once the first patch has been calculated, the algorithm queries the aircraft for its current location in order to determine whether the aircraft has traveled into the first patch. Upon entering the patch, the algorithm updates by using the following equations:

$$\vec{X}_{p_2} = \vec{X}_{D1}(t_u + t_h) \tag{5}$$

$$\vec{X}_{p_{i+1}} = \vec{X}_{Di}(t_h), \qquad i = 2,3,4,... \tag{6}$$

where

$\vec{X}_{Di}$ Dynapath trajectory for the ith patch

t_h HUD pathway display length

The algorithm selects a point corresponding to the time required for the computational cycle time, t_u, plus the time corresponding to the length of the pilot's pathway-in-the-sky display, t_h, in the initial patch (eq. 5). Next, using equation 6, the path prediction is accomplished by using the desired trajectory position at t_h, thus requiring the initial segment of the trajectory to come from the two previously calculated patches. In this way, the algorithm update is imperceptible to the pilot.

Trajectory Coupler

After the Dynapath algorithm produces its optimal trajectory it is passed to the trajectory coupler. The trajectory is represented by 30 discrete instances of commanded aircraft-inertial state (position, velocity, and acceleration) at 1-sec intervals. Also stored are commanded bank angles, headings, and vertical flight-path angles. The trajectory coupler converts the quantized commanded trajectory into a trajectory command that is designed to work synchronously with the pilot displays at a minimum of 20 Hz, thus not imposing any time-delay that is perceptible to the pilot. This is accomplished by interpolating within the trajectory to determine the instantaneous position of the trajectory points that are to be presented on the pilot's head-up-display.

Displayed Information

The guidance and control information was displayed to the pilot on a Flight Dynamics head-up-display (HUD) in the format shown in figure 4. The HUD is framed by four triangular symbols directed at the center of the display. Since the HUD is body-fix mounted, these symbols represent the pitch and roll axes reference. The primary situational information is presented to the pilot with a flight-path vector/predictor symbol, represented by the circular aircraft icon. The logic that drives this symbol will be discussed later. Digital airspeed and radar altitude are attached to the flight-path vector/predictor symbol on the left and right, respectively. A longitudinal acceleration cue (>) and airspeed flight director, in the form of a tape, are likewise attached. The horizon line along with pitch reference lines are presented in a conventional way. The situational information presented on the HUD in figure 4 indicates that the pilot is turning right with a slight descent as indicated by the flight-path vector/predictor below the horizon.

The trajectory command information on the HUD is given by the pathway-in-the-sky and phantom aircraft. The pathway symbols represent a three-dimensional perspective of the commanded inertial position and heading of the discretized commanded states. The phantom aircraft is displayed on the HUD as a delta-wing aircraft. The phantom aircraft represents the instantaneous position along the commanded trajectory that is 3 sec ahead of the pilot's aircraft. The phantom aircraft attitudes also are derived from the commanded trajectory, using the commanded vertical flight-path angle, commanded bank, and commanded heading as pitch, roll, and yaw, respectively. As discussed

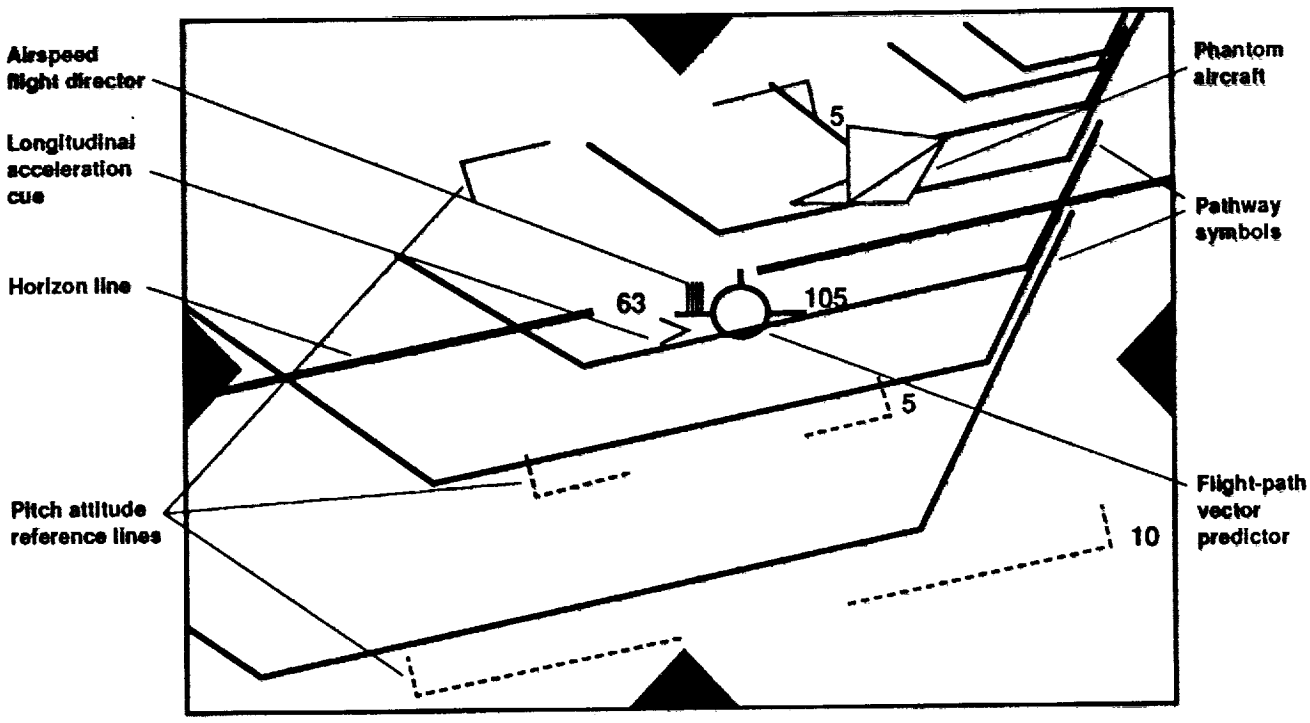

Figure 4. HUD format.

in reference 13, by positioning the flight-path vector symbol on the phantom aircraft, the pilot will track the desired trajectory; this technique is referred to as pursuit tracking. In figure 4, the HUD is commanding a climbing right turn.

The pathway is 100 ft wide at the bottom with vertical projections that are canted at a 45° angle; the width at the top is 200 ft. The depth of the path is 50 ft below the intended trajectory; thus, when flying a level straight-line commanded path, the pilots used the analogy of traveling in a full irrigation canal for describing the pathway symbols. To avoid unnecessary clutter, the pathway was restricted to only the next 7 sec of flight.

The pathway always represented the actual commanded trajectory on the HUD. Thus, if the trajectory was not visible in the field of view (FOV) of the HUD (±10° vertically and ±15° horizontally), then the pathway likewise was not displayed. However, if the phantom aircraft position is outside the FOV, the symbol is positioned on the edge of the HUD closest to the true position so that the pilot will know the direction to the path even though he cannot see it. At this point the positioning of the flight-path vector/predictor symbol relative to the phantom aircraft will remain true. The relative position between the two symbols is the error term for pilot tracking and is no longer situational data. This change in mode is indicated to the pilot by blinking the vector/predictor symbol at a rate of once per second.

The primary guidance information is provided by the phantom aircraft symbol and the flight-path vector/predictor symbol. The vertical flight-path vector/predictor γ_{vp} is driven by

$$\gamma_{v_p} = \gamma_v + \frac{\tau_H s}{\tau_H s + 1}\left(K_{\delta_c}\delta_c + \theta\right) \tag{7}$$

where

γ_v vertical flight-path angle

τ_H aircraft heave time-constant

s Laplace operator

K_{δ_c} collective input gain (0.095 rad/in)

δ_c collective stick input (inches)

θ pitch attitude (rad)

The horizontal flight-path vector/predictor γ_{H_p} is driven by

$$\gamma_{H_p} = \gamma_H + \frac{T_p A_y / V}{1 + \sqrt{1 - (T_p A_y / V)^2}} \tag{8}$$

where

γ_H horizontal fight-path angle

T_p prediction time (3 sec)

A_y lateral inertial acceleration

V helicopter's velocity

The vertical predictive term is compensated for the heave-time constant of the aircraft. Since the simulated helicopter's flight-control system produces vertical velocity in response to collective input, the collective feedback gives the pilot an immediate feedback of his control actions to the aircraft vertical flight-path angle. Therefore, the pilot can position the flight-path symbol vertically without waiting for the aircraft to respond. The horizontal prediction term integrates along path curvature to determine where the aircraft will be 3 sec later based on the aircraft's current inertial acceleration (ref. 14). Therefore, the pilot can position the flight-path vector/predictor on the phantom aircraft with little difficulty.

SIMULATION FACILITY AND TEST PROCEDURE

The piloted simulation was conducted on the Ames Research Center six-degree-of-freedom Vertical Motion Simulator (VMS). The VMS provides extensive cockpit motion for use in studying the handling qualities of, and the advanced guidance concepts for, existing and proposed aircraft (ref. 15). The VMS and the operational limits of the motion system are shown in figure 5. The cockpit visual scene with the HUD and head-down moving-map display is shown in figure 6. The cockpit was configured with conventional cyclic, collective and pedal controls. The visual system, a Singer Link digital image generator, consists of a four-window display of computer-generated imagery (CGI). Figures 7(a)-7(c) show a planner view of the CGI data base used for the simulation with three different waypoint sets. The first waypoint set (fig. 7(a)) was used to test the terrain following feature of the guidance algorithm; the second set (fig. 7(b)) was used to test the terrain avoidance; and the third set (fig. 7(c)) was used to test an equal mixture.

The data base consists of a central area with pyramid-shaped hills (with altitudes up to 1,000 ft), trees, and buildings. Leading into the central area are three sets of parallel, 3,000-ft-long, inverted-V-shaped peaks (prism shaped). Some of these peaks have 200-ft-wide notches or valleys cut into them. The hill sets were chosen to give the trajectory-generation algorithm a clear choice for the generation of the optimal trajectories and to provide a comparison with a previous simulation in which the pilot task was primarily terrain-following (refs. 16 and 17). A digital terrain-map, representing an advanced DMA format of the data base, was made with a 10-m resolution and with terrain altitude quantized to 10 m, for use by the guidance algorithm. Additionally the data base was seeded with trees and houses up to 60 ft high. These obstacles were not available to the Dynapath algorithm for trajectory calculation.

The helicopter mathematical model used during the development and evaluation of the system concept is detailed in reference 18. The model characteristics and dynamics are very similar to those of a UH-60 flown at light weight. The pilots flew the aircraft using conventional collective, cyclic, and pedal controls by using an attitude-rate and vertical-velocity-command flight-control system. The model is based on a simple six-degree-of-freedom, nonlinear, stability-derivative, point-mass model. The helicopter model also had a simulated autopilot with full trajectory-coupling and airspeed-hold modes. These two modes were used primarily for pilot demonstrations and training.

Ten helicopter pilots representing NASA, the U.S. Army, and the U.S. Air Force participated in the evaluations. A total of 302 simulation runs were conducted with an average run covering 8 to 12 n.mi. over extremely varying terrain. The test matrix is shown in table 1.

The evaluations consisted of a baseline case (waypoint set 2, an airspeed of 60 knots, a ground set-clearance of 100 ft, a maximum bank command of 17°, no turbulence, and unlimited visibility) and the eight variations shown in table 1. The variations included the other waypoint sets, varying speeds (40 and 90 knots), a lower set-clearance (40 ft above ground level (AGL)), an increased maximum bank command (30°), inclusion of moderate turbulence, and reduction of visibility to 0.25 mile. The pilot started each run with the trajectory guidance information displayed on the HUD and with the helicopter trimmed at the correct altitude, heading, and airspeed for the commanded trajectory.

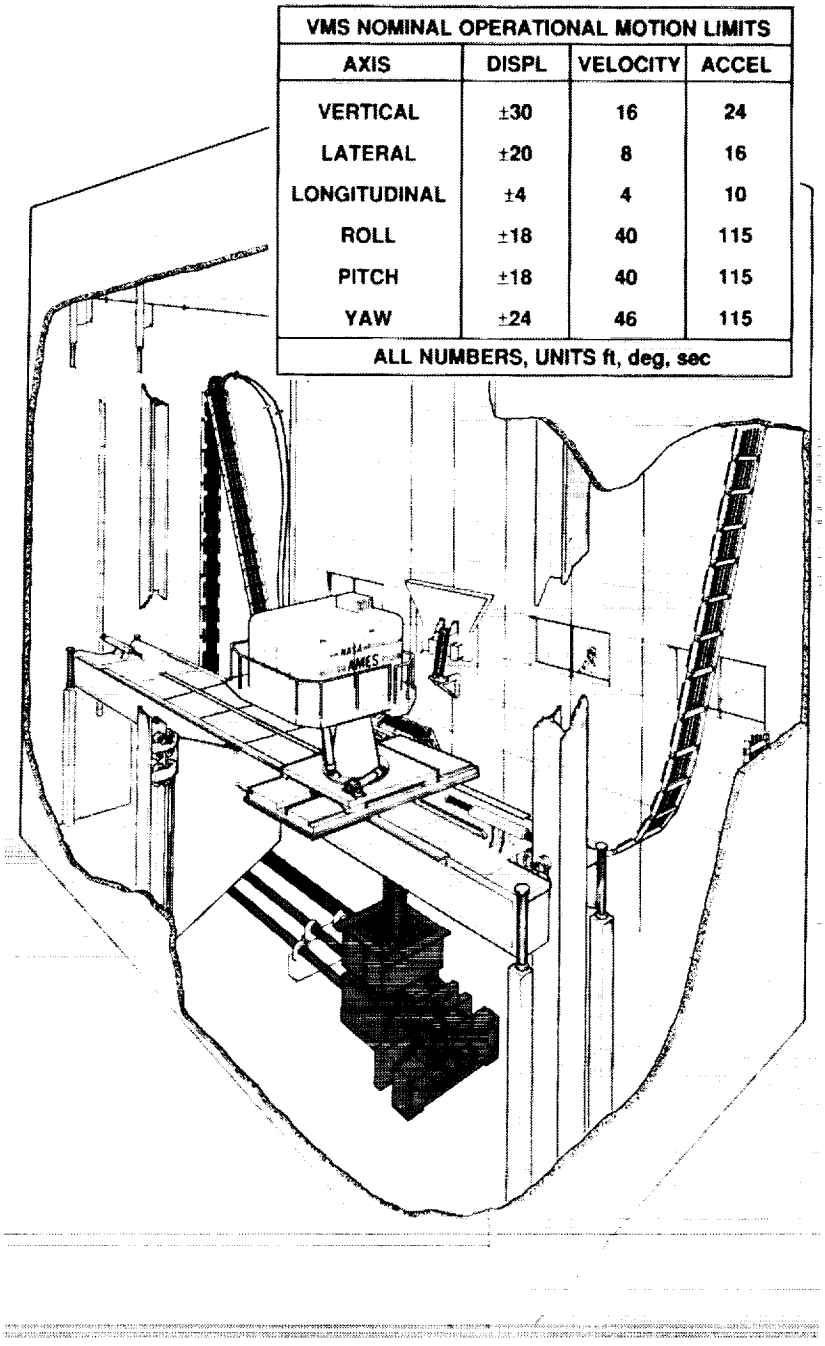

Figure 5. Vertical Motion Simulator.

ORIGINAL PAGE
BLACK AND WHITE PHOTOGRAPH

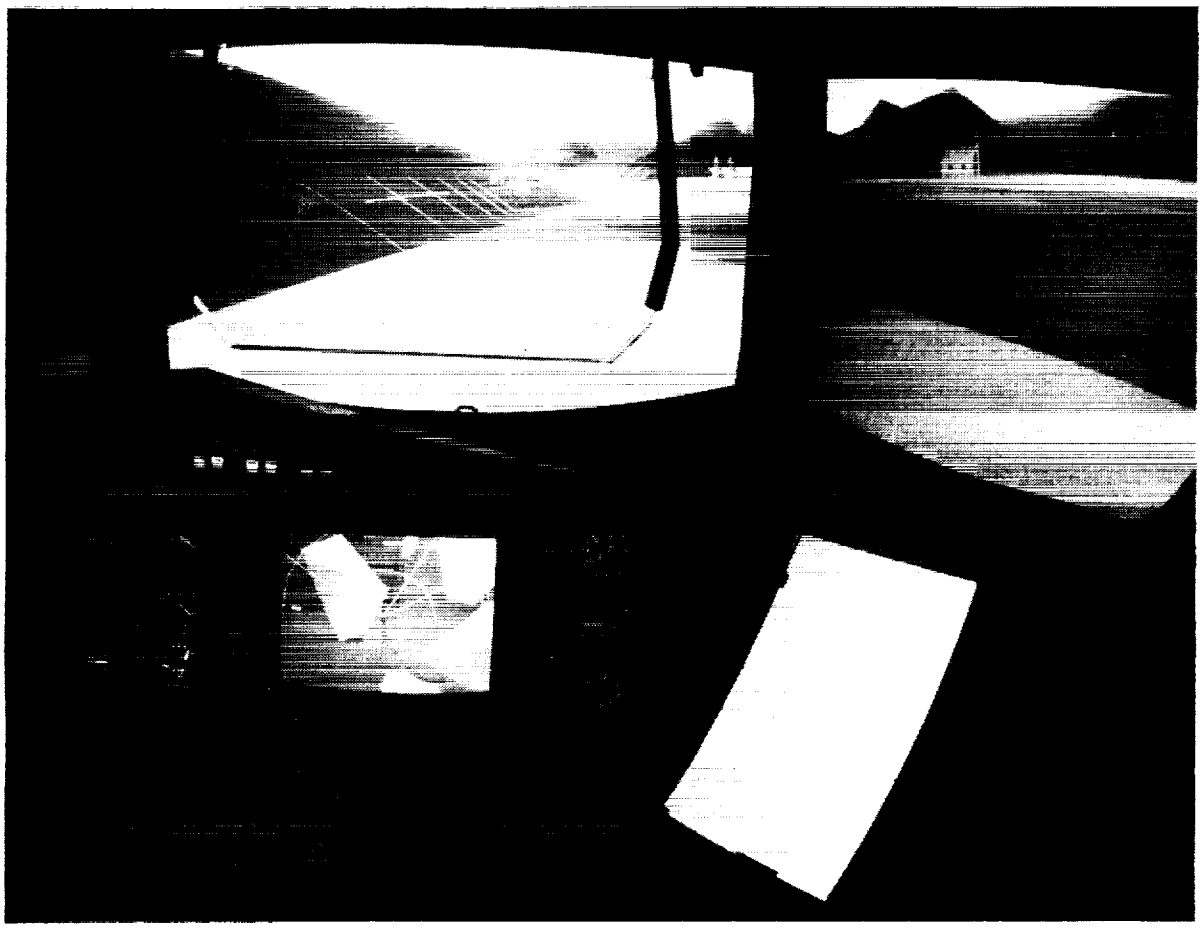

Figure 6. Cockpit visual scene.

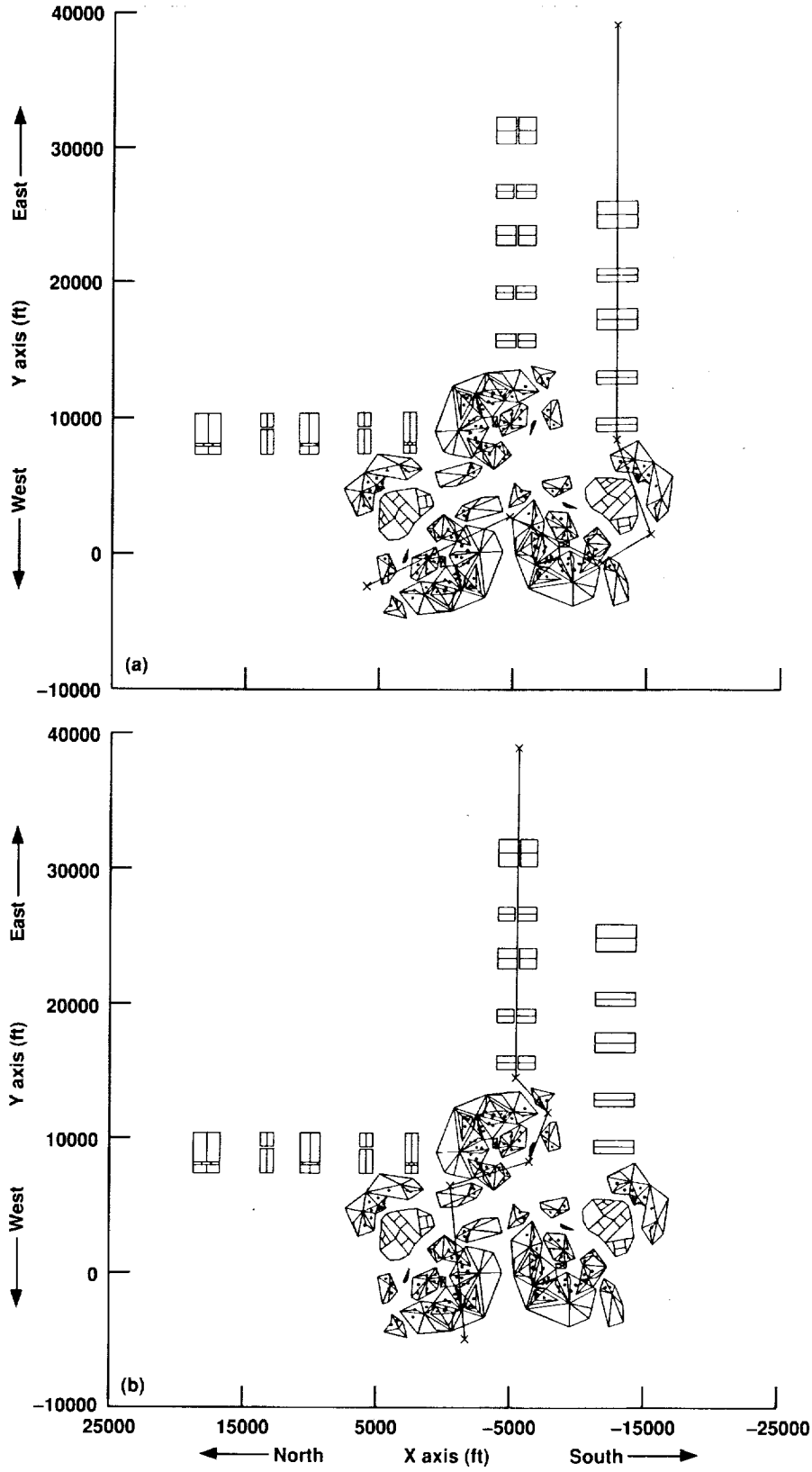

Figure 7. Computer-generated-imagery data base. a) Waypoint set 1; b) waypoint set 2.

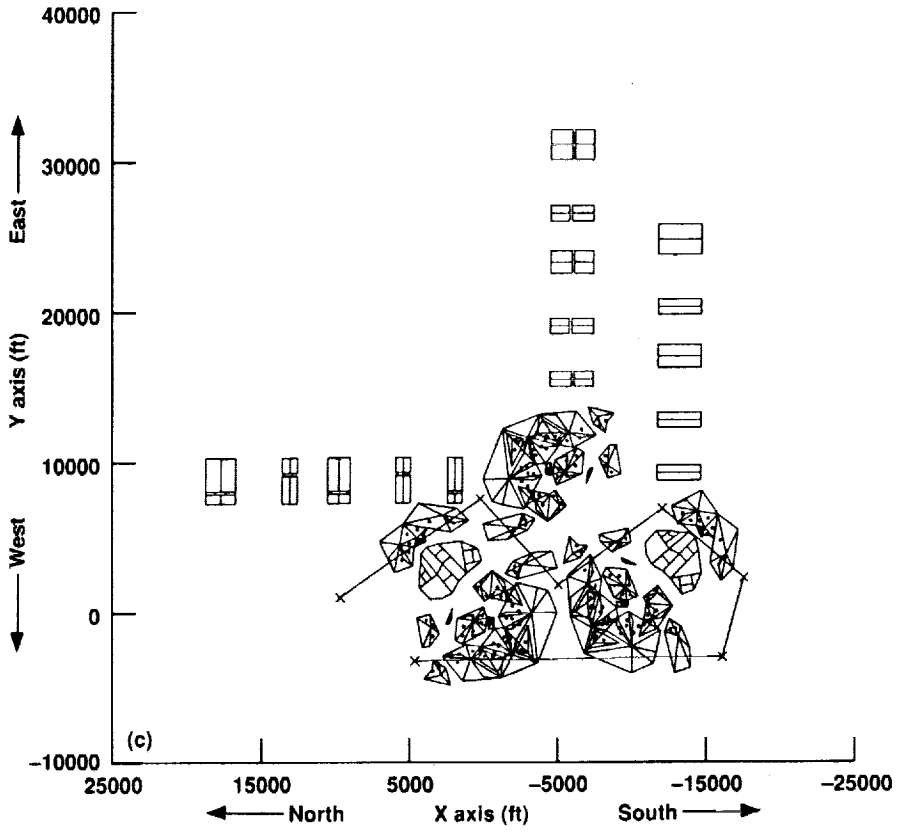

Figure 7. Concluded. c) Waypoint set 3.

Table 1 Simulation test matrix

Configuration	Waypoint set	Airspeed, knots	Set-clear, ft, AGL	Maximum bank command, deg	Turbulence (moderate)	Visibility
Baseline	2	60	100	17	Off	Unlimited
1	1	60	100	17	Off	Unlimited
2	3	60	100	17	Off	Unlimited
3	2	40	100	17	Off	Unlimited
4	2	80	100	17	Off	Unlimited
5	2	60	40	17	Off	Unlimited
6	2	60	100	30	Off	Unlimited
7	2	60	100	17	On	Unlimited
8	2	60	100	17	Off	1/4 mi

The pilot was given two kinds of tasks. For the 100-ft AGL set-clearances (table 1), the task was to precisely follow the flight-path vector/predictor and phantom aircraft guidance to determine flight technical error. For the 40-ft AGL set-clearance, the pilot was asked to use the guidance for general navigation but to override the command as required for obstacle avoidance. This is a fundamentally different task.

RESULTS AND DISCUSSION

For all the test combinations listed in table 1 the pilots were able to maintain very precise guidance tracking using the flight-path vector/predictor and phantom aircraft display. Lateral and vertical pilot guidance-tracking performance plots are shown in figure 8(a)-8(d) for the baseline case. The figures display tracking performance as a function of distance traveled along waypoint set 2. Figure 8(a) is a composite of lateral guidance tracking of all the simulated runs for the test condition. Figure 8(b) shows the mean and 1-σ (standard deviation) lateral tracking error also as a function of distance traveled. In figures 8(c) and 8(d) the composite and statistical vertical tracking performance capability is shown as a function of distance traveled. These plots are shown as representative of the pilot tracking performance for the test configurations.

The lateral and vertical pilot guidance tracking errors for all configurations are summarized in figure 9. The figure shows 1-σ pilot tracking performance as a function of each configuration tested. As evident, with the exception of the 40-knot case, the 30° maximum commanded bank-angle case, and the 40-ft AGL set-clearance case, the vertical and lateral tracking performance was under 6 ft. There is some degradation, 3 ft to 6 ft, in lateral performance as the guidance shifted from TF to TA to TF/TA; this can be attributed to the increased lateral maneuvering. The configuration for environmental effects, for example, turbulence and limited visibility, showed results similar to the baseline configuration and represented no significant piloting difficulties.

In the slow-speed and maximum bank command of 30° configurations, the pilots seemed to have greater difficulty tracking the guidance. This is attributed to the fact that in both these cases the guidance generates lateral maneuvers by using increased path curvature, as can be seen from equation 1. Additionally, in the slow-speed case the helicopter is just starting transitional lift, thus making its basic handling qualities worse.

As discussed earlier, the pilot's task when flying the low set-clearance altitude was somewhat different from the other cases. For the low set-clearance altitude (40 ft AGL), the pilot was flying at the resolution accuracy of the digital-terrain data base and at the altitude of trees and buildings within the data base that are not included in the guidance algorithm. For this reason the pilots were instructed to only use the guidance as an aid and to manually avoid obstacles and terrain that were in the commanded trajectory. All the pilots successfully avoided the obstacles within the data base. It is interesting to note that the pilots usually chose lateral maneuvering to avoid the obstacles. This is evident by comparing the lateral deviation from the commanded path (31 ft, 1-σ) with the lateral tracking error measured in the baseline case (8 ft, 1-σ). This is due to the pilot initiating maneuvers around obstacles and then tracking back to the commanded path. The vertical tracking performance

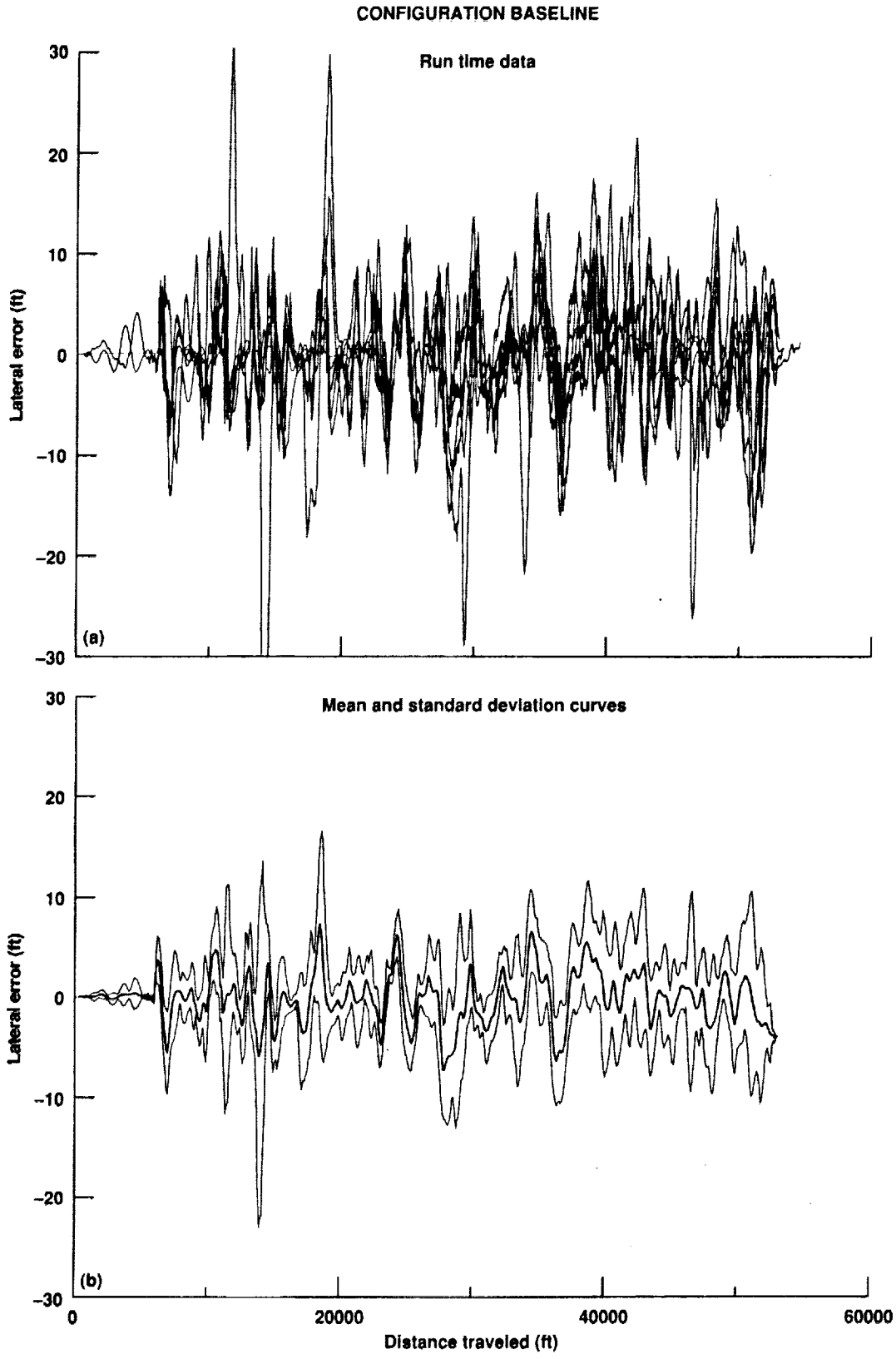

Figure 8. Pilot guidance-tracking performance baseline configuration. a) Composite of lateral tracking on all runs; b) mean and 1-σ lateral error.

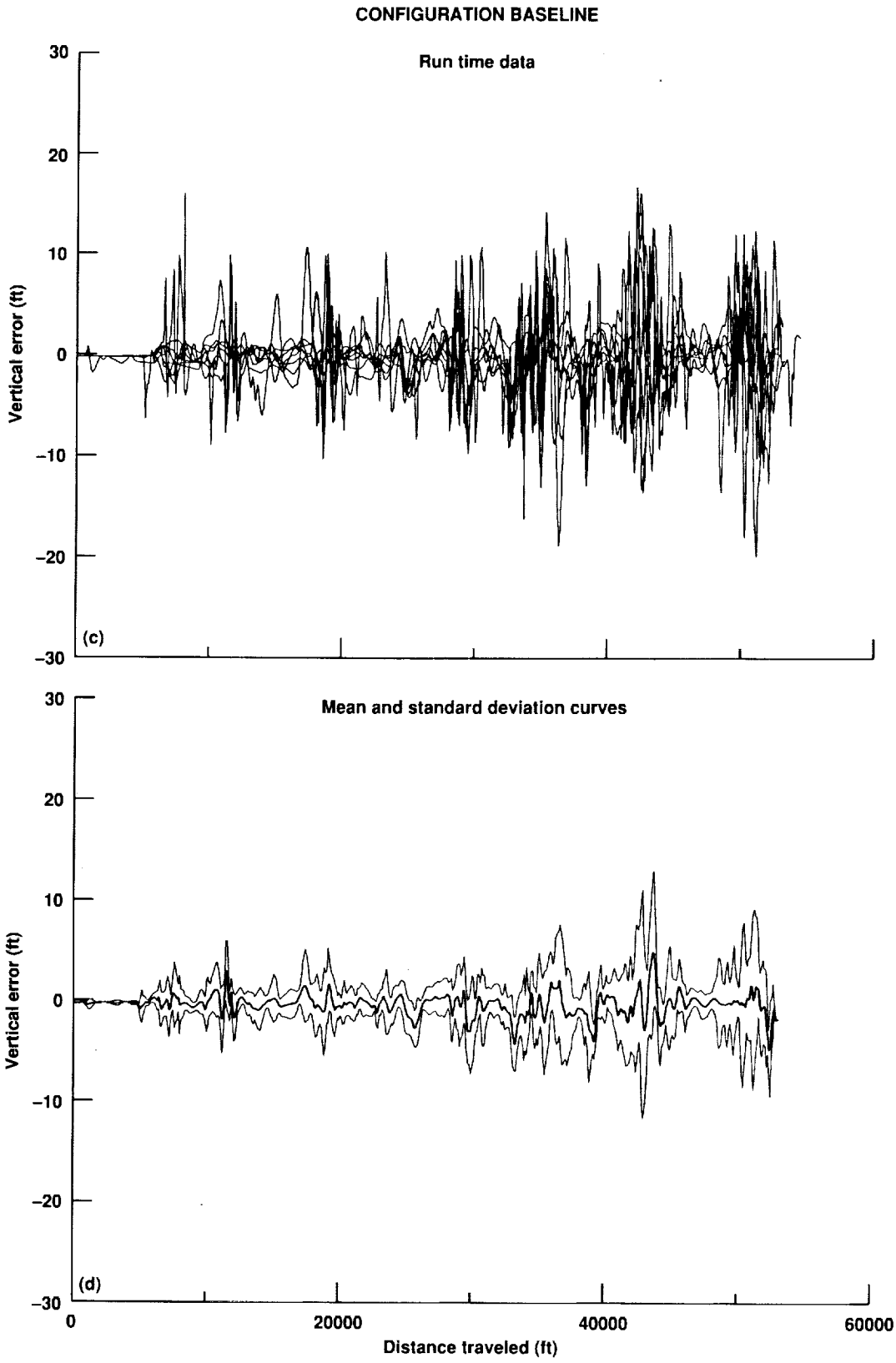

Figure 8. Concluded. c) Composite of vertical tracking on all runs; d) statistical vertical performance.

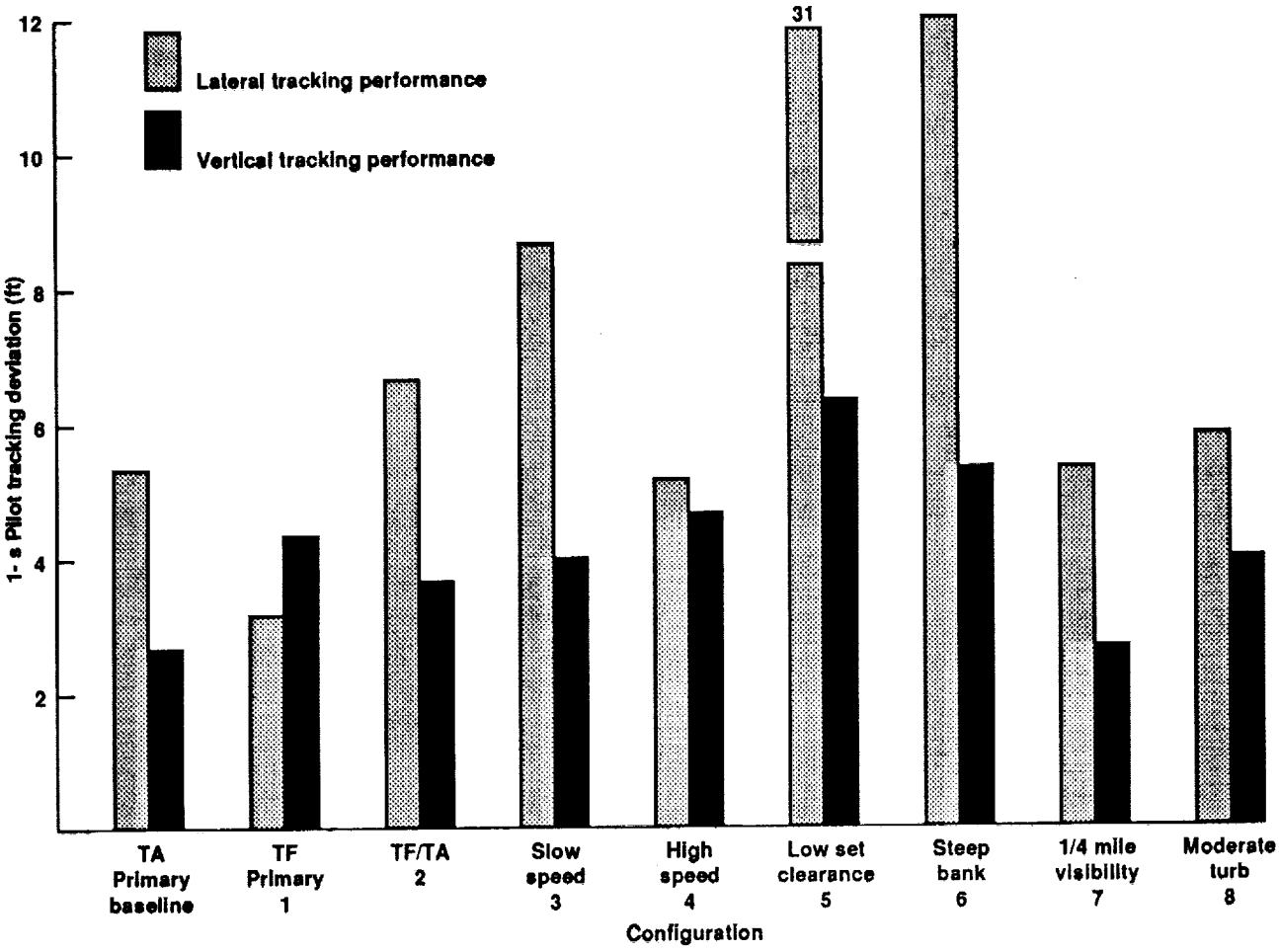

Figure 9. Pilot tracking performance: summary.

(10 ft, 1-σ) is very similar to the baseline configuration (8 ft 1-σ), thus implying that lateral maneuvering was the first choice among the pilots for manual obstacle avoidance.

In simulation debriefings, the pilots indicated that the system was easy to fly, predictable, and demonstrated an ability to provide a safe flyable trajectory at low altitudes. A major operational attribute of the display presentation, as identified by the pilots, is the ease with which they can depart from and reacquire the commanded path. This feature was viewed as being particularly useful in intermittently changing visibility conditions where the pilot may choose to leave the commanded trajectory for improved concealment when visibility is good but wants to reacquire the trajectory as visibility degrades. They also commented upon the ease with which they could effectively use the guidance for general navigation information while they were manually avoiding obstacles for flight at very low altitudes.

Based on pilot acceptance of the concept, a joint NASA/Army program has been initiated to test the concept in flight. Ames Research Center is working with the U.S. Army Avionics Research and Development Activity at Ft. Monmouth, to install the system in the UH-60 STAR (Systems Testbed

for Avionics Research) helicopter. The flight test will use a Honeywell IHADSS helmet-mounted display and head-tracker instead of the HUD. This integration is proceeding and is scheduled for flight test in 1992.

CONCLUSIONS

A low-level, maneuvering penetration guidance algorithm for helicopter operations has been developed and evaluated in a full-motion simulator. The evaluation pilots were able to manually track the HUD guidance through various combinations of terrain, speeds, and weather that were representative of system use. The guidance is easy to follow without detracting from the pilot's awareness of the outside world. The pilot is able to combine the guidance with his own sightings to optimize the mission success in varying weather/threat conditions. The computer-aiding concept has matured as a single system development through the extensive use of piloted simulation. The integration of the concept into flight is the next logical step. Plans for this project are currently progressing through a joint NASA/Army program on the UH-60A STAR helicopter.

REFERENCES

1. Tripp, E.: SOF Helicopters: Operating on the Dark Side. Rotor & Wing International, Dec. 1987.

2. Wendl, M. J.; Katt, D. R.; and Young, G. D.: Advanced Automatic Terrain Following/Terrain Avoidance Control Concepts Study. NAECON Conference Proceedings, 1982.

3. Russ, D. E.; Houtz, J. E.; and Rothstein, S. W.: Evaluations of Alternative Terrain Following/ Terrain Avoidance (TF/TA) Systems Designs Using Pilot in the Loop Simulation. AGARD CP-387, Oct. 1985.

4. Denton, R. V.; Jones, J.; and Froeberg, P. L.: A New Technique for Terrain Following/Terrain Avoidance Guidance Command Generation. AGARD CP-387, Oct. 1985.

5. Nordmeyer, R.: Enhanced Terrain Masked Penetration. Final Technical Report, AFWAL TR-86-1079, Sept. 1986.

6. Dorr, D. W.: Rotary Wing Aircraft Terrain Following/Terrain Avoidance System Development. NASA TM-88322, 1986.

7. Hoffman, J. D.: Terrain-Following/Terrain-Avoidance/Threat-Avoidance for Helicopter Applications. AHS Proceedings National Specialists' Meeting in Rotorcraft Flight Controls and Avionics, Oct. 1987.

8. Pekelsma, N. J.; and Denton, R. V.: Pilot Oriented Aids for Helicopter Automatic Nap of the Earth Flight. AHS Proceedings National Specialists' Meeting in Rotorcraft Flight Controls and Avionics, Oct. 1987.

9. Swenson, H. N.; Hardy, G. H.; and Morris, P. M.: Simulation Evaluation of Helicopter Terrain Following/Terrain Avoidance Concepts. AIAA Paper 88-39224-CP, 1988.

10. Denton, R. V.; Froeberg, P. L.; Jones, J. E.; and Nikoukhah, R.: Terrain Following/Terrain Avoidance Algorithm Study. AFWAL TR-85-3007, May 1985.

11. Denton, R. V.; Pekelsma, N. J.; and Smith, F. W.: Autonomous Flight and Remote Site Landing Guidance Research for Helicopters. NASA CR-177478, 1987.

12. Pekelsma, N. J.; and Smith, F. W.: Optimal Guidance with Obstacle Avoidance for Nap-of-the-Earth Flight. NASA CR-177515, 1988.

13. Bray, R.; and Scott, B.: A Head Up Display for Low Visibility Approach and Landing. AIAA Paper 81-0130, 1981.

14. Grunwald, A. J.: Predictor Laws for Pictorial Flight Displays. AIAA Journal of Guidance, Control, and Dynamics, Sept.-Oct. 1985.

15. Jones, A. D.: Operations Manual: Vertical Motion Simulator (VMS) S.08. NASA TM-81180, 1980.

16. Swenson, H. N.; Paulk, C. H.; Kilmer, R. L.; and Kilmer, F. G.: Simulation Evaluation of Display/FLIR Concepts for Low-Altitude Terrain-Following Helicopter Operations. NASA TM-86779, 1985.

17. Kilmer, F. G.; Kilmer, R. L.; Swenson, H. N.; and Woodward, A. C.: A Helicopter Terrain Following System for Terminal Area Operations. AIAA Paper 85-3092 AIAA/AHS/ASEE Aircraft Design Systems and Operations Meeting, Oct. 1985.

18. Lewis, M. S.; Mansur, M. H.; and Chen, R. T.: A Piloted Simulation of Helicopter Air Combat to Investigate Effects of Variations in Selected Performance and Control Response Characteristics. NASA TM-89438, 1987.

NASA
National Aeronautics and Space Administration

Report Documentation Page

1. Report No.	2. Government Accession No.	3. Recipient's Catalog No.
NASA TM-103861		

4. Title and Subtitle	5. Report Date
Computer Aiding for Low-Altitude Helicopter Flight	May 1991
	6. Performing Organization Code

7. Author(s)	8. Performing Organization Report No.
Harry N. Swenson	A-91140
	10. Work Unit No.
	505-64-36

9. Performing Organization Name and Address	11. Contract or Grant No.
Ames Research Center Moffett Field, CA 94035-1000	
	13. Type of Report and Period Covered
12. Sponsoring Agency Name and Address	Technical Memorandum
National Aeronautics and Space Administration Washington, DC 20546-0001	14. Sponsoring Agency Code

15. Supplementary Notes

Point of Contact: Harry N. Swenson, Ames Research Center, MS 210-9, Moffett Field, CA 94035-1000, (415) 604-5469 or FTS 464-5469

Report presented at the 47th Annual Forum of the American Helicopter Society, Phoenix, AZ, May 6-8, 1991

16. Abstract

A computer-aiding concept for low-altitude helicopter flight has been developed and evaluated in a real-time piloted simulation. The concept included an optimal control trajectory-generation algorithm based on dynamic programming, and a head-up display (HUD) presentation of a pathway-in-the-sky, a phantom aircraft, and flight-path vector/predictor symbol. The trajectory-generation algorithm uses knowledge of the global mission requirements, a digital terrain map, aircraft performance capabilities, and advanced navigation information to determine a trajectory between mission waypoints that minimizes threat exposure by seeking valleys. The pilot evaluation was conducted at NASA Ames Research Center's Sim Lab facility in both the fixed-base Interchangeable Cab (ICAB) simulator and the moving-base Vertical Motion Simulator (VMS) by pilots representing NASA, the U.S. Army, and the U.S. Air Force. The pilots manually tracked the trajectory generated by the algorithm utilizing the HUD symbology. They were able to satisfactorily perform the tracking tasks while maintaining a high degree of awareness of the outside world.

17. Key Words (Suggested by Author(s))	18. Distribution Statement
Low-altitude helicopter flight, Helicopters, Pilot displays, Terrain following, Terrain avoidance	Unclassified-Unlimited Subject Category - 04

19. Security Classif. (of this report)	20. Security Classif. (of this page)	21. No. of Pages	22. Price
Unclassified	Unclassified	24	A02